# Investigation of interface grading in MOVPE grown GaAs/GaAlAs quantum well heterostructures using photoluminescence measurements

M. S. S. Loural and M. T. Furtado
*Centro de Pesquisa e Desenvolvimento, Telecomunicações Brasileiras S/A - TELEBRAS, C.P.1579, Campinas, 13.088-061, SP, Brazil*

and

M. A. Sacilotti
*IUT-GMP and LPS, Université de Bourgogne, B.P. 138, 21004, Dijon, France*

Recebido em 22 de novembro, 1996

The compositional grading at the interfaces of GaAs/$Ga_{1-x}$ $Al_x$As ($x$=0.15-0.41) quantum well (QW) heterostructures grown by atmospheric pressure MOVPE, were investigated with photoluminescence (PL) spectroscopy. The interface grading was determined by adjusting the calculated optical transition of the ground state emission, with the associated PL peak position measured from QW heterostructures samples comprising various QWs with different well widths (10-160 Å), but having the same barrier height. The compositional grading profile was assumed to vary linearly at the QW interfaces, and the calculated optical transitions were obtained by solving the Schroedinger equation employing numerical methods, under the assumption of the envelope function approximation. The interface grading width was found to increase with the Al content in the barrier layers, and the rate measured in QW heterostructures with high Al content in the barriers was 2% of Al per Å. However, no grading was detected in QW heterostructures grown with low Al content in the barriers. The evaluation of the interface compositional grading was found to be primarily limited by uncertainties in the QW thickness measurements, but it is still very precise compared to other techniques.

A composição gradual das interfaces em heteroestruturas com poços quânticos (PQs) de GaAs/$Ga_{1-x}Al_x$As ($x$=0.15-0.41) crescidos pela técnica MOVPE à pressão atmosférica, foram investigadas com a espectroscopia de fotoluminescência (FL). A gradualidade nas interfaces é determinada pelo ajuste do cálculo das transições ópticas fundamentais com a posição dos picos associados de FL medidos em heteroestruturas constituidas de vários PQs com espessuras diferentes (10 - 160 Å), mas com a mesma composição de Al nas barreiras. Consideramos o modelo linear para a variação do perfil de composição gradual de Al nas interfaces, e efetuamos os cálculos das transições ópticas através da resolução da equação de Schroedinger por métodos numéricos na aproximação da função envelope. Observou-se um aumento da gradualidade nas interfaces com a composição de Al nas camadas das barreiras, medindo-se uma taxa de 2% de Al por Å nas heteroestruturas de PQs com alta composição de Al nas barreiras. No entanto, não detectamos nenhuma gradualidade nas interfaces de heteroestruturas crescidas com baixa concentração de Al nas barreiras. A principal limitação na determinação da gradualidade nas interfaces reside nas incertezas das medidas de espessura dos PQs, porém o método apresentado é ainda bastante preciso comparado com outras técnicas experimentais.

## I. Introduction

In the last years, quantum size effects in semiconductor heterostructures of III-V materials have been intensively investigated due to the wide interest for applications in photonic and electronic devices[1,2]. For instance, quantum well (QW) semiconductor lasers have been fabricated with better performances than conventional double heterostructure lasers, as demonstrated by the lower threshold currents, the higher power and efficiencies, as well as the greater modulation bandwiths. These benefits originate from the two dimensional staircase density of states[3], which improve the device characteristics and also opens new possibilities to adjust the emission wavelength by control of the QW width. The great advancement of QW heterostructure devices fabricated with the GaAs/GaAlAs material system, results from the large improvements obtained with two epitaxial growth techniques: Metalorganic Vapor Phase Epitaxy (MOVPE) and Molecular Beam Epitaxy (MBE). Abrupt interfaces in the atomic scale with good thickness control and uniformity are now routinely grown with these techniques, which also favoured considerable progress in electronic devices, such as heterojunction bipolar transistors[4,5], field effect transistors[6], and resonanat tunneling diodes[7].

The study of QW interfaces has been an active field of research since the discovery of QW heterostructures. Photoluminescence (PL) spectroscopy has emerged as an important tool for the analysis of QW heterostructures grown by MBE[1,8−12] and MOVPE[13−23]. The PL technique extracts basic physical parameters of QW heterostrucures, such as the ground state transition energy and the QW width, where the latter is usually determined from adjustments with theoretical predictions. Moreover, the full width at half maximum (FWHM) of the PL emission delivers important information about the roughness of QW interfaces[24,25]. A complete and extensive review about the study of QW interface roughness employing different luminescence techniques has been presented by Herman et al[26]. Besides, the RHEED (reflection high energy electron diffraction) analysis generally employed in the MBE growth system, other techniques are also employed in the characterization of QW interfaces, such as high resolution X-ray diffraction[27], and more recently, atomic force spectroscopy[28] and cross-sectional scanning tunneling microscopy[29]. The investigation of abrupt QW interfaces, is a an active research field in GaAs/$Ga_{1-x}Al_xAs$ heterostructures grown with different substrate orientations[7,12,27].

Nevertheless, there is an increasing interest for QW heterostructures with compositional grading at the interfaces[30−34]. Most often, the grading results from thermal interdiffusion induced by vacancies or impurities, either during growth or as a post-growth process. The change produced in the QW emission wavelength has been intensively investigated because opens new possibilities as a technological processing step for device applications. The adjustment of calculated optical transitions with PL data has been generally performed for large amounts of compositional grading using either error function[30−32] or linear profiles[33,34]. However, small compositional grading widths of the order of only a few monolayers, still remain quite unexplored[21−23]. These may occur during the MOVPE growth process, as the result of the gas switching system or the hydrodynamic gas flow in the reactor chamber. Some previous attempts have been reported with Auger electron spectroscopy (AES)[35,36], but presenting poor resolution for small grading widths.

In this work, we have investigated the compositional grading of GaAs/$Ga_{1-x}Al_xAs$ QW heterostructure interfaces grown by atmospheric pressure MOVPE using PL spectroscopy. A systematic study was undertaken using samples grown with different Al content in the barrier layers ($x$=0.15-0.4) incorporating multiple QWs of different widths. A theoretical treatment based on the envelope function approximation was undertaken in order to determine the ground state emission wavelength, employing a linear symmetric grading compositional profile at both QW interfaces. The PL technique detects compositional grading widths of only a few monolayers, which cannot be detected by any direct compositional profile measurements. This study was carried out during the optimization process of a home built MOVPE system. The compositional grading at the QW interfaces was primarily attributed to the gas residence time in the reactor chamber, which originates from dead space volumes in the Al gas switching valve, and consequently, affects the Al gas switching flow. In addition, we have also monitored the FWHM from the PL peaks of the QW heterostructures.

In section II, we present the model used to determine the Al compositional grading of the QW interfaces of the GaAs/$Ga_{1-x}Al_xAs$ heterostructures. The experimental details of the MOVPE growth and PL measurements are described in section III. Section IV describes the PL results as well as the interface grading analysis, and section V presents the results and discussion of the FWHM obtained from the PL spectra. Finally, in section VI, the conclusion is presented.

## II. Theory

The theoretical aproach used for modeling the compositional grading at the interfaces of QW heterostructures, based on the envelope function approximation[37,38], is summarized below. The growth direction is defined as the $z$-axis, in which the layers have finite dimension. For simplicity, we consider a single QW heterostructure with a GaAs ultrathin layer confined by two $Ga_{1-x}Al_xAs$ layers. Since the PL emission involves only the lowest allowed energies for electrons and holes in the QW layer, the ground state transition energy is given by the expression:

$$E_{lh} = E_g^A + E_e^l + E_{hh}^l \tag{1}$$

where $E_e^l$ and $E_{hh}^l$ denote the first energy level for electrons in the conduction band and heavy holes in the valence band, respectively.

In the envelope function approximation, the Schroedinger equation for electrons and holes in the QW heterostructure can be simplified by solving the Ben Daniel-Duke Hamiltonian[39] for the respective envelope functions in the $z$ direction:

$$\left\{ -\frac{\hbar}{2}\frac{\partial}{\partial z}\frac{1}{m_l(z)}\frac{\partial}{\partial z} \right\} \chi_l(z) = E\chi_l(z) \tag{2}$$

where $V$ is the potential energy, $\chi$ is the particle wavefunction, $l$ is the band index for heavy holes ($hh$) and light holes ($lh$) in the valence band or electrons ($e$) in the conduction band. The effective mass $m_l(z)$ is a function of position in the $z$ axis. It takes the GaAs material value in the QW region and the $Ga_{1-x}Al_xAs$ material value in the barriers. The origin of the energies is at the bottom of the conduction band and at the top of the valence band for electrons and holes, respectively.

In a simple square QW with abrupt interfaces, $E_e^l$ and $E_{hh}^l$ are easily determined by the transcendental equation for the even solutions of $\chi_l(z)$ given in refs.[37,38]. When the QW interfaces present a finite width or grading $G$ extending over a few monolayers, a change is expected in the magnitude of the QW energy levels $E_e^l$ and $E_{hh}^l$. In a GaAs QW confined by $Ga_{1-x}Al_xAs$ barrier layers, we define $G$ as the extension in the $z$-axis corresponding to the interval from the barrier where the Al concentration decreases from $x$ (when the Al valve in the MOVPE reactor is closed) until it reaches zero and, inversely, to the distance where the Al composition increases from zero to $x$ when the valve is opened again. Other investigators[22,23] have applied exponential functions to describe hypothetical graded wells, but without fitting the experimental data. We have previously considered error function profiles for modeling large interface grading produced by interdiffusion of Ga-Al in GaAs/GaAlAs QWs[30] and of In-Ga in InGaAs/GaAs QWs[31]. In the present work, we have assumed a simple model of linearly graded and symmetric interfaces as shown in figure 1, because it results in a greater simplification of the theoretical calculations and also describes reasonably well the experimental data.

As pointed out by Delalande and Bastard[40], the results are independent of the exact shape of the grading as long as the grading of the interfaces are smooth. Figures 1-a and 1-b show the widths ($L_z$) of a square QW and a gradual QW, respectively, where the grading is defined as the average width at the middle of the barrier height. The ground state energies $E_e^l$ and $E_{hh}^l$ increase with the interface grading $G$, resulting in a shift of the $E_{lh}^l$ PL peak transition energy given by equation (1) to higher values relative to the square QW. When $G$ is larger than $L_z$ the shape of the QW structure becomes triangular with some residual Al concentration at the center of the well ($z = 0$), and consequently the QW band gap also increases.

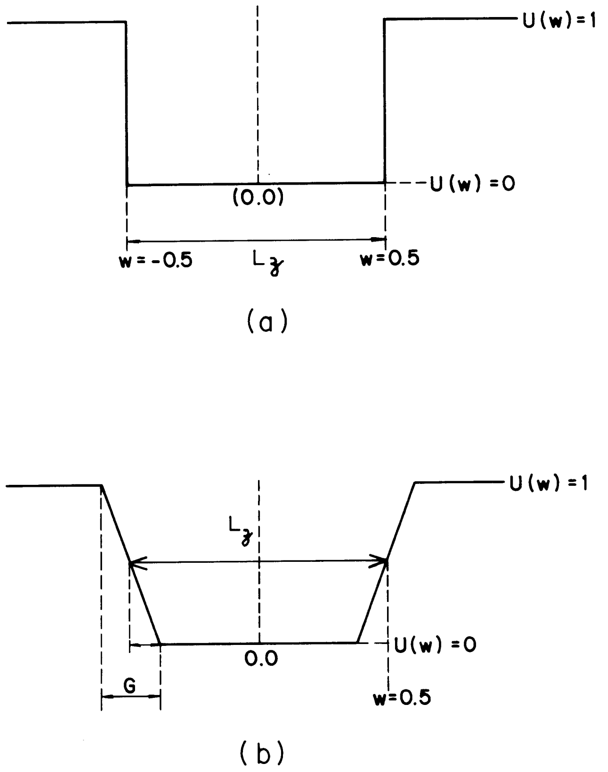


Figure 1: Energy band diagram in dimensionless units: (a) square QW heterostructure and (b) QW heterostructure with linear compositional grading at the interfaces.

The Ben Daniel-Duke Hamiltonian for electron and holes cannot be solved analytically in compositionally graded QW heterostructures, thus it is more convenient to write equation (2) in terms of the dimensionless variables $w$, $U(w)$ and $\epsilon_n$ as indicated in figures 1-a and 1-b:

$$\left\{\frac{d}{dw}\frac{1}{m(w)}\frac{d}{dw}\right\}\phi_n(w) = \frac{2L_zV}{\hbar^2}\{U(w)-\epsilon_n\}\phi_n(w) \tag{3}$$

where, $w = z/L_z$, $\epsilon_n = E_n/V$, and $U(w) = V(z)/V$. Here $V = V_s$ and $E_n = E_e^n$ for electrons in the conduction band, and $V = V_p$ and $E_n = E_{hh}^n$ for heavy holes in the valence band.

The differential equation (3) can be solved as a difference equation[41]. The $w$-axis is divided into intervals $\Delta w$, and the position $w_j$ is given by $w_j = j\Delta w$. The function $U(w)$ retains the information about the grading in dimensionless units, such that $g$ represents the number of intervals $\Delta w$ in which $U(w)$ goes from zero to one, or $V(z)$ goes from zero to $V$. We then have $G = g \times L_z \times \Delta w$.

Equation (3) can now be written as:

$$\phi_n(w_{j+1}) = \left\{1 - \frac{2VL_z^2m_{j+1}(\Delta w)^2}{\hbar^2}[\epsilon_n - U(w_j)]\right\}$$

$$\phi_n(w_j) + \frac{m_{j+1}}{m_j}\{\phi_n(w_j) - \phi_n(w_{j+1}\} \tag{4}$$

It can be observed in equation (4) that if we know the values of $\phi_n(w_j)$ and $\phi_n(w_{j-l})$ for a given value of $\epsilon_n$, we can determine $\phi_n(w_{j+1})$, $\phi_n(w_{j+2})$ and so on by an iteration procedure. So, equation (4) can be solved by assuming the same values of $\phi_n(w_0)$ and $\phi_n(w_1 = \Delta w)$ as for the square QW. This is a good approximation since no modifications are expected for the wavefunction at the center of the QW near $w = 0$, since the potential variation only occurs at the interfaces where $w = 0.5$. Therefore, the grading $G$ will be determined by the value that makes the wavefunction converge to zero when $w$ approaches $\pm\infty$ for both electrons and holes, for given values of $L_z$ and the measured PL peak energy in equation (2), respectively. The energy gap at 77K and the effective masses used in the calculations were taken from ref.[42], except for the hole effective mass of GaAs[43]:

$$m_e^{GaAs} = 0.0665m_0$$

$$m_{hh}^{GaAs} = 0.34 m_0$$

$$m_e^{GaAlAs} = (0.0665 + 0.083x) m_0$$

$$m_{hh}^{GaAlAs} = (0.34 + 0.31x) m_0$$

$$E_g^{GaAs}(eV) = 1.507$$

$$E_g^{GaAlAs}(eV) = 1.507 + 1.247x$$

where $m_0$ is the free electron mass. The conduction band offset was taken as 0.4 [44]. We have also considered the energy dependence for the electron effective mass in the conduction band, which is given by [45]:

$$m_e^{GaAs} = (0.0665 + 0.0436E + 0.236E^2 - 0.147E^3) m_0$$

### III. Experimental procedure

The samples studied in this work were grown in a home made atmospheric pressure MOVPE reactor. More details of our growth system are described in refs. [36,46,47]. The samples consisted of 4 or 5 GaAs QW layers of different widths, confined by 500 Å thick $Ga_{1-x}Al_xAs$ barrier layers. The QW widths and the Al content in the barrier layers were in the range $L_z = 10 - 160$ Å and $x = 0.15 - 0.41$, respectively. Each sample had constant growth rate and Al content in the barriers. The growth time being different for each QW, starting from the largest and ending with the smallest QW, from substrate to surface. The structures were grown on < 100 > oriented undoped GaAs substrates followed by a 2 $\mu$m thick GaAs buffer layer. The general scheme is shown in figure 2. The epitaxial layers were nominally undoped and $n$-type. The carrier concentrations measured on thicker layers grown under the same conditions were $n = 2 \times 10^{14}$ cm$^{-3}$ for GaAs, whereas in $Ga_{1-x}Al_xAs$, $n$ increased from $5 \times 10^{15}$ cm$^{-3}$ to $5 \times 10^{16}$ as $x$ was raised from 0.15 to 0.41. The growth rate for GaAs and $Ga_{1-x}Al_xAs$ layers was 10 Å/sec for all samples except for one with 5 Å/sec. The QWs growth time sequence was 16, 8, 4 and 2 seconds for all samples except for the one with the lower growth rate with 32, 16, 8, 4, and 2 seconds. The growths were carried out at a temperature of 700 °C with a III/V ratio of 50 optimized to obtain GaAs layers with the best quality. Switching of the reactor valves was manual with no interruptions at the interfaces. The QW widths were estimated from the relation $L_z = \nu t$, where $\nu$ is the growth rate extrapolated from the growth calibration of thicker layers and $t$ is the growth time. This relation was checked by a direct thickness measurement using the scanning electron microscope (SEM). The measurement was carried out on a 20 period multi-QW GaAs/$Ga_{1-x}Al_xAs$ ($x$=0.3) heterostructure having a nominal QW and barrier layer thickness of 100 Å and 500 Å, respectively. The SEM measurement resulted in a thickness of 93 Å for each QW layer, which corresponds to a 7% deviation from the value estimated by the relation $L_z = \nu t$. The multi-QW structure presented a narrow PL peak with a FWHM of 9 meV [48], confirming the repeatability of the QW layers growth in our MOVPE system.

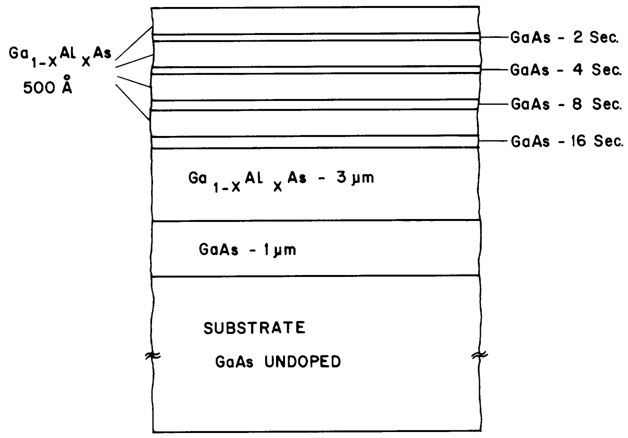


Figure 2: Schematic diagram of the growth sequence of the QW heterostructure samples.

The samples were analysed by PL in liquid nitrogen at 77K. They were excited with the 5145 Å Argon laser line. Neutral density filters were placed in the beam path in order to obtain a power of 5 mW, focused in a 500 $\mu$m spot diameter onto the sample (2.5 W/cm$^2$). The PL emission was focused into a 25 cm spectrometer with a 0.1 mm entrance slit, corresponding to 3 Å or 0.5 meV resolution for the GaAs region.

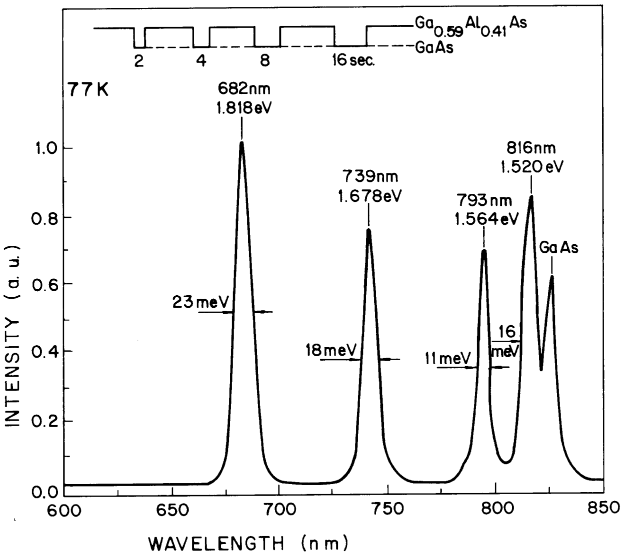


Figure 3: 77 K PL spectra of a heterostructure with 4 QWs and 41 % Al content in the barrier layers. The lowest energy peak at 850 nm is from the GaAs buffer layer. The inset shows the the conduction band diagram with the growth time for each QW layer.

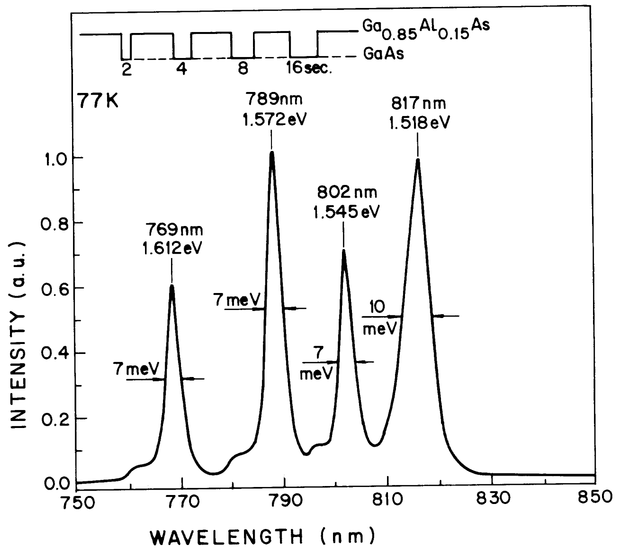


Figure 4: 77 K PL spectra of a heterostructure with 4 QWs and 15 % Al content in the barrier layers. The high energy shoulders visible on the emission peaks correspond to the electron to light hole transitions. The inset shows the conduction band diagram with the growth time for each QW layer.

## IV. Results and analysis

Our first observations of the PL ground state emission $E_{lh}$ in QW heterostructures with large Al content in the barrier layers ($x \approx 0.4$), indicated a systematic high energy shift deviation from the calculated values for a perfect square QW. On the other hand, no shift was observed on heterostructures with low Al content in the barrier layers ($x \approx 0.15$). AES profiles measured on similar samples showed that heterostructures with high Al content presented a strong evidence of residual Al in the smaller QWs, while the same result was not confirmed on heterostructures with low Al content because of resolution limitations in the AES technique[35,36,48]. In order to further investigate this behaviour, we proceeded to make a systematic 77 K PL study on samples with similar structures to that shown in figure 2, but varying the Al content in the barrier layers. In figures 3 and 4, we present the PL spectra of QW heterostructures with 41 % Al and 15 % Al content in the barrier layers, respectively. The PL peak positions correspond to the ground state emission from the QWs in each structure. In a previous study, we have shown that the PL peaks are uniform over an area about 12 cm$^2$ [46].

In figures 5 and 6, we have plotted the PL peak wavelengths ($\lambda$) from the QW heterostructures shown in figures 3 and 4, respectively, as a function of the nominal QW thicknesses ($L_z$). In the same figures are shown the 77 K calculated theoretical curves of $\lambda$ versus $L_z$, where $\lambda = hc/E_{lh}$. The solid lines shown on both figures, correspond to calculations using the potential function of a perfect square QW with abrupt interfaces, and the dashed line shown in figure 5 was obtained with a linear compositional grading profile for the QW interfaces as described in section II. The Al molar fraction $x$ used in the calculations was determined by the PL peak position of the $Ga_{1-x}Al_xAs$ barrier layer. The $Ga_{1-x}Al_xAs$ emission could be easily distinguished from the emission of the QWs because the former presented the lowest intensity and the largest FWHM, localized at the high energy side of the PL spectra.

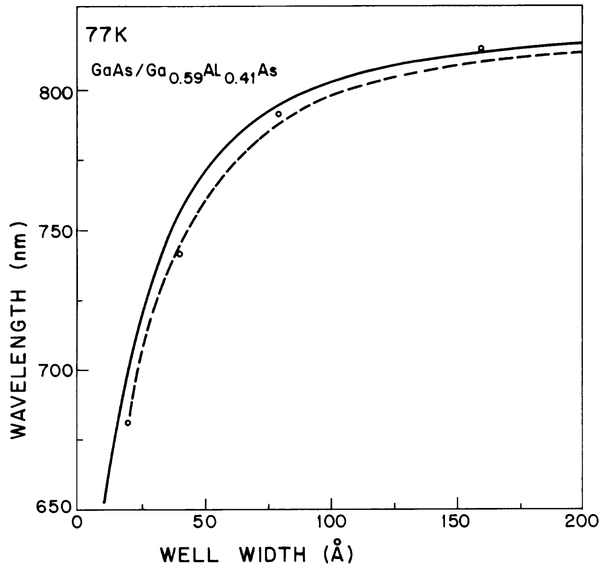


Figure 5: Plot of the PL peak wavelengths ($\lambda$) versus QW width ($L_z$) for the sample shown in figure 4. The calculated optical transitions are shown as the solid line for a square QW heterostructure, and as the dashed line for a QW heterostructure with linear compositional grading at the interfaces ($G$ = 20 Å).

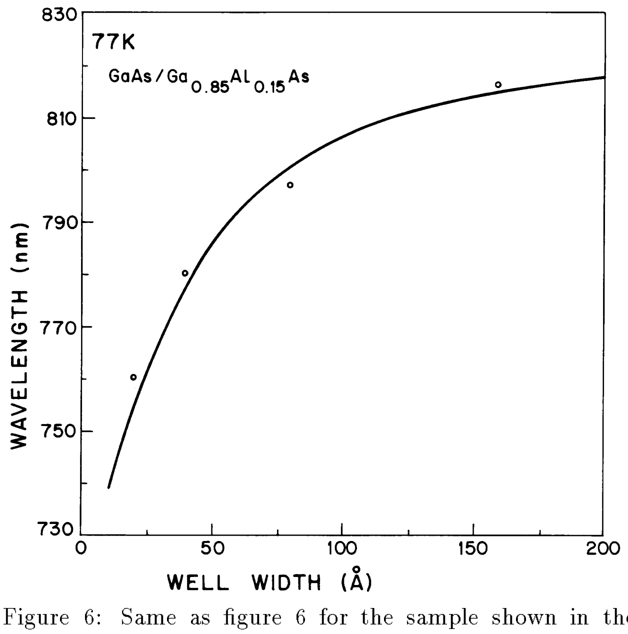


Figure 6: Same as figure 6 for the sample shown in the figure 5. The solid line corresponds to calculated optical transitions for a square QW heterostructure.

One notices on figure 6 that the experimental data is satisfactorily represented by the calculated optical transitions obtained for QWs with abrupt interfaces. On the other hand, one observes on figure 5, except for the largest QW width, a systematic shift to lower wavelengths of the PL peak values relative to the calculated transitions with abrupt interfaces. The dashed line shown on this figure was obtained by assuming the same compositional interface grading $G$ = 20 Å for all QWs. This is a plausible assumption for our samples, since the interfaces are primarily smeared by the gas residence time in our MOVPE reactor[46]. The value of $G$ = 20 A corresponds to the minimum root mean square deviation from the experimental data relative to the calculated dashed line, within an interval $G = (20 + 2)$Å. Hence, the grading uncertainty in this measurement is of the order of one monolayer thickness (2.8 Å).

We have studied five samples in this work which are summarized in table 1. Samples 1 and 5 are those shown in figures 4 and 3, respectively. Following the same procedure described for sample 5, we have obtained for the other samples the results shown in table 1. One notices from table 1 that the interface grading is larger with increasing Al content in the barrier layers, and that a residual amount of Al is expected at the center of the smaller QWs when $L_z < G$, as demonstrated in our first AES observations[36,48]. From the results of samples 3, 4 and 5 we can approximate the Al decay or increase rate as 2 % Al per Å unit. For lower barriers (less than $x$ = 0.25) we cannot detect any grading. The values for the interface grading presented in table 1, are within a range of one monolayer thickness, very precise and cannot be obtained by other techniques. The major uncertainty results from the QW thickness evaluation through the relation $L_z = \nu t$. We can estimate the uncertainty in the determination of $G$ if we assume a +7 % error in our $L_z$ measurements, as determined by the SEM analysis described in section III. By repeating the optical transitions calculations with $L_z + 0.07L_z$, we can evaluate the corresponding uncertainty in $G$. This calculation was done for sample 5 which presents the largest compositional grading. We obtained the value $G = (20 \pm 5)$ Å, which corresponds to an uncertainty of about 3 monolayers thickness in the grading measurement, although we might expect that t may also influence somewhat the thinner QWs (10-20 Å), because of the manual gas switching flow employed in our MOVPE system. We have performed other measurements on samples with nominal $L_z = 100$ Å, aiming to check the sample uniformity. The thickness estimated from the plot of $\lambda$ versus $L_z$, similar to the ones shown in figures 3 and 4, were in the range $L_z = (97.5 \pm 4.5)$ Å over an area about 12.5 cm$^2$. This mean value of $L_z$ must be considered within the $\pm 7\%$ uncertainty thickness deviation obtained for the SEM measurements described in section III.

*Table* 1: Parameters of the QW heterostructure samples

| *Sample* | *Al content in the barriers* | *Number of wells* | *Growth rate* (Å/s) | *Grading* (Å) |
|---|---|---|---|---|
| 1 | 0.15 | 4 | 10 | 0 |
| 2 | 0.25 | 4 | 10 | 0 |
| 3 | 0.37 | 5 | 5 | 15 |
| 4 | 0.37 | 4 | 10 | 15 |
| 5 | 0.41 | 4 | 10 | 20 |

On the other hand, samples 3 and 4 grown with the same Al content in the barrier layers, but with different growth rates, have apparently the same grading at the QW interfaces. This result is not clearly undertood, because it depends on the growth dynamics near the substrate in the MOVPE system, which is beyond the scope of this work. However, we may speculate a possible explanation by assuming a simple diffusion limited growth process, which controls the gas residence time, and consequently, the grading. The growth rate is primarily limited by mass transport of the column *III* reactant gases through the vapour phase adjacent to the substrate[49]. In fact, the mass transport process is quite complex, because it involves the hydrodynamics of the carrier gas flow as well as the diffusion across the laminar flow near the substrate. Nevertheless, the growth rate is controled by the slower diffusion process, which is proportional to the input partial pressure of the column *III* reactant gases[50]. The same is expected to occur with the gas residence time, which should increase as the input partial pressure is lowered. Then, the overall effect might produce a grading independent of the Al partial pressure and the growth rate, as shown for samples 3 and 4 in table 1.

We must point out here that we did not consider the exciton binding energy in our calculations, since we have assumed that the PL emission in the QWs occurs from transitions between the conduction and valence bands. In fact, the contribution of excitons to the PL emission around liquid nitrogen and higher temperatures is still a matter of debate among different investigators. Hermann et al.[26] presented a detailed discussion of undoped QWs showing that excitonic transitions are predominant in the PL emission spectrum. This is supported by the observation of PL linewidths smaller than the thermal energy kT in high quality QWs[51,52]. Nevertheless, Ping[53] reported more recently, assuming a mass action law formalism, that free and bound excitons are affected by the presence of free carriers, and consequently, contribute less to the PL intensity, consistent with other experimental data. This was confirmed later by PL transient measurements[54], where an increasing nonexponential bimolecular decay was observed as the temperature increased from very low values. Besides, previous reports on MOVPE grown QWs, did not consider excitons as remaining bound at 77K, because the exciton binding energy is of the same order as kT [22,55]. The exciton binding energy of undoped GaAs/GaAlAs QWs have been reported by several authors, and usually range from 9-12 meV to 6-9 meV as the width increases from 30 Å to 100 Å, respectively[22,26]. Moreover, as the carrier density increases, the exciton binding energy decreases because of carrier screening, many body exchange and correlation effects[56,57].

Our QW samples grown with low Al content in the barriers have low carrier concentrations, so we have assumed that the PL peak emission involves primarily free carriers with some minor contributions from free and bound excitons, where the latter transitions somewhat increase the PL FWHM. Since the QW samples grown with high Al content in the barriers have larger carrier concentrations, the exciton binding energy is consequently reduced, and we have therefore neglected any excitonic contribution to the PL emission.

## V. PL FWHM as a function of QW width

Figure 7 shows the FWHM of the PL peak as a function of the QW width ($\Delta E$ versus $L_z$) for all samples shown in table 1. Our $\Delta E$ values are about 20 % higher than those reported by Kawai et al[22] for samples with higher barriers ($x = 0.54$). The well known PL broadening mechanisms for QW structures are: fluctuations in the QW width, interface roughness[25], alloy composition variation at the interfaces[58] and band filling[59]. As shown on figure 7, we found that the band filling is the predominant broadening mechanism for the PL FWHM of samples with higher Al content in the barrier layers. The band filling mechanism consists in a carrier transfer from donors in the confining layers into the QW layers, turning the semiconductor degenerated inside the QWs and shifting the Fermi level higher than the first quantum level. According to Welch et al[59] the band filling mechanism is described by the expression:

$$\Delta E = \frac{n_z \pi^2 \hbar^3}{L_z m_e (2 m_e E_e)^{1/2}} \tag{5}$$

where $n_e$ is the sheet carrier density in the QW layers, $m_e$ is the electron effective mass, and $E_e$ is the electron energy relative to the bottom of the conduction band.

In figure 7, the solid curve represents the band filling mechanism calculated from equation (5). $E_e$ was derived from the calculations described in section II. For the samples with $x = 0.41$ and $x = 0.37$ in the barrier layers, we found a good fit using $n_s = 1.8 \times 10^{11}$ cm$^{-2}$. Subtracting the thermal energy $kT$ (6.7 meV at 77 K) from the $\Delta E$ values, we obtain $n_s = 1.2 \times 10^{11}$ cm$^{-2}$, which corresponds to a transfer of a bulk carrier density of 2.4 × $10^{16}$ cm$^{-3}$ from the $Ga_{1-x}Al_xAs$ barrier layers with a thickness of 500 Å. This result is in a reasonable agreement with the value of 5 × $10^{16}$ cm$^{-3}$ obtained from Hall effect and electrochemical C-V measurements on thicker $Ga_{1-x}Al_xAs$ layers, where the residual carrier density was found to increase with the Al content in the layers[36].

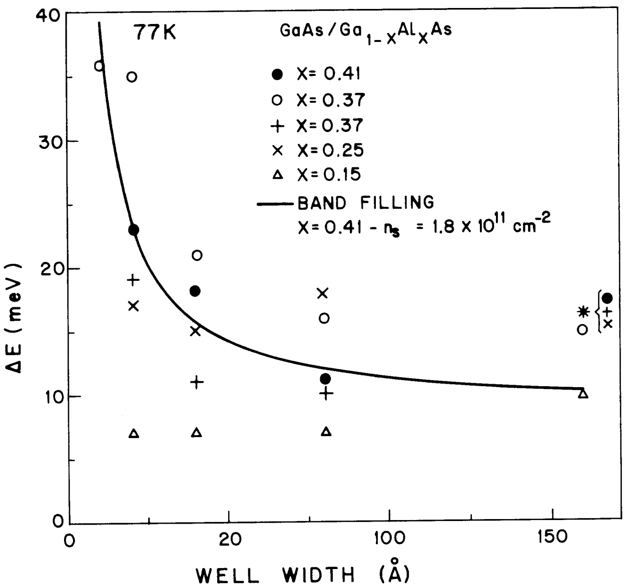


Figure 7: Plot of the PL FWHM ($\Delta E$) versus $L_z$. The solid line represents the band filling mechanism with $n_s$ = 1.8 × $10^{11}$ cm$^{-2}$ and $x = 0.41$.

Except for the sample with $x$=0.15, one notices from figure 7 that the larger QWs (160 Å) present a systematic deviation for higher $\Delta E$ values. This additional increase of $\Delta E$ might be attributed to a slight superposition of the QW peak with the very near GaAs buffer layer emission peak, as seen in the spectra of figure 3, which apparently presents only a minor contribution on the sample grown with $x$=0.15 (figure 4). On the other hand, the influence of the band filling mechanism decreases as expected, for samples with lower barriers. This fact is consistent with a smaller carrier transfer from the barriers due to the lowering of the residual carrier density as the Al content decreases in the barrier layers. As we can see in figure 7, QWs with 15 %

Al content in the barrier layers present a constant PL FWHM, which is the same as kT at 77K (6.7 meV), indicating good quality for the interfaces in the QWs. The sample with 25 % Al barrier layers presents an unusual behaviour that cannot be explained by simply changing the $n_s$ value or any of the mechanisms presented above, and neither by a combination of them. This behaviour is not clearly understood, but may be probably caused by fluctuations of the growth conditions for this sample.

One must also consider that other mechanisms such as QW width fluctuations of the order of few monolayer steps cannot be discarded from our samples. Statistical calculations[25] and experimental measurements[26] have shown a strong correlation between the extension of a fixed value of $L_z$ in the QW plane (island) and the PL linewidth from excitonic transitions at low temperatures. The PL peak is narrow for islands smaller than the exciton diameter, but $\Delta E$ increases when the extension of the islands become similar to the exciton diameter and decreases again for larger values. These results were mostly reported on samples grown by MBE, but were also observed on samples grown by MOVPE, where the size of the islands increase with the growth interruption time at the QW interfaces[26]. In our QW heterostructures, we have probably very small islands because there was no growth interruption at the interfaces. However, the islands may increase in size as the growth rate decreases, which is consistent with the larger $\Delta E$ values obtained with the sample grown with the lower growth rate in figure 7. But, as pointed out above, we have not considered any contribution from excitons in the PL spectra of QW heterostructures grown with higher Al content in the barrier layers.

Finally, the value of $n_s$ obtained from the band filling mechanism suggests that band gap renormalization effects might be significant in the QW layers of heterostructures with high Al content in the barrier layers[57,60]. We can estimate the expected shift to lower energies using the simple expression of Kleinman and Miller, which reads $E_{BGR}$ (meV) $= 2\ C(n_s)^{0.32}$ with $C = 2.2 \times 10^{-3}$ meV.cm$^{0.64}$ and where $E_{BGR}$ is the band gap renormalization energy for the annihilation of the electron-hole pair[60]. If we assume $n_s$ equal to $1.2 \times 10^{11}$ cm$^{-2}$, we obtain $E_{BGR}$ around 15.4 meV, so that the measured PL peaks shown in figure 3 are somewhat shifted to longer wavelengths about 6 to 8.4 nm as $L_z$ increases from 20 to 160 Å, respectively. Therefore, the PL peaks of the two larger QWs shown in the figure should be closer to the calculated curve for the gradual interface, while the corresponding PL peaks of the thinner QWs should be shifted farther to lower wavelengths. However, this effect has little influence on our results, and is inherent only to the residual carrier concentration of our samples with high Al content in the barrier layers.

## VI. Conclusions

We have undertaken a systematic study of a series of MOVPE grown $Ga_{1-x}Al_xAs/GaAs$ ($x = 0.15-0.41$) QW heterostructures with different QW widths and Al content in the barrier layers using 77 K PL measurements. We have calculated the PL peak wavelength of the ground state emission versus QW width ($\lambda \times L_z$) for square as well as graded QWs. The departure of the PL data from theoretical predicted values for an ideally perfect QW heterostructure with abrupt interfaces, allowed us to determine the interface grading that best fits the PL measurements. Although a simple symmetric linear compositional grading profile was assumed for the QW interfaces, the grading measurements are quite precise and limited only by the uncertainty in the QW width, which was estimated as $\pm 7$ % in our samples. The results obtained show that the interface grading in our QW heterostructures increases with the Al content in the barrier layers. A grading of $(20 \pm 5)$ Å was obtained for 41% Al content in the barrier layers, with a variation rate of the Al concentration about 2% Al per Å. However, on QW heterostructures grown with low Al content in the barriers ($x = 0.15$), no grading was detected at the interfaces. The PL measurements are non destructive, and are more precise than alternative direct measurement profile techniques usually employed for determining the compositional grading profile of QW interfaces.

Finally, the method described in this work for measuring the compositional grading of QW interfaces, can be extended to other III-V compound materials systems, such as InGaAs/InP and InGaAs/InAlAs/InP QW heterostructures[48]. In this case, the method is not straightforward as for the GaAs/GaAlAs system, because the ternary InGaAs alloy in the QWs can be strained by a small amount from the lattice matched composition. This fact causes a positive or negative PL peak shift that depends on the strain (compressive or tensile), resulting in an uncertainty in the energy gap value which may influence the grading estimative.

### Acknowledgement

One of the authors (M.S.S. Loural) acknowledges financial support during part of this work from the Conselho Nacional de Desenvolvimento Científico e Tecnológico (CNPq).

### References

1. H. Okamoto, Japan. J. Appl. Phys. **26**, 315 (1987).
2. H. Heinecke and E. Veuhoff, Mater. Sci. Eng. B **21**, 120 (1993).
3. Y. Arakawa and A. Yariv, IEEE J. Quantum Electron. **22**, 1887 (1986).
4. P. M. Asbeck, M. C. F. Chang, J. A. Higgins, N. H. Sheng, G. J. Sullivan and K. C. Wang, IEEE Trans. Electron. Dev. **36**, 2032 (1989).
5. S. Tanaka, M. Ito, M. Ikeda and T. Kikuta, J. Cryst. Growth **124**, 812 (1992).
6. M. A. Tischler, D. Latulipe, T. F. Kuech, J. H. Magerlein and H. J. Hovel, J. Cryst. Growth **124**, 824 (1992).
7. M. Shinohara, H. Yokohama and N. Inoue, J. Vac. Sci. Technol. B **13**, 1773 (1995).
8. K. Fujiwara, K. Kanamoto, N. Tsukada, H. Miyatake and H. Koyama, J. Appl. Phys. **66**, 1488 (1989).
9. K. Brunner, G. Abstreiter, G. Bohm, G. Trankle and G. Weimann, Appl. Phys. Lett. **64**, 3320 (1994).
10. W. Liu, D. Jiang, K. Luo, Y. Zhang and X. Yang, Appl. Phys. Lett. **67**, 679 (1995).
11. S. Hiyamizu, S. Shimomura, A. Wakejima, S. Kaneko, A. Adachi, Y. Okamoto, N. Sano and K. Murase, J. Vac. Sci. Technol. B **12**, 1043 (1994).
12. T. Yamada, H. Yamaguchi and Y. Horikoshi, Japan. J. Appl. Phys. **35**, L822 (1996).
13. R. D. Dupuis, J. G. Neff and C. J. Pinzone, J. Cryst. Growth **124**, 558 (1992).
14. D. C. Bertolet, J. K. Hsu and K. M. Lau, J. Appl. Phys. **64**, 6562 (1988).
15. R. T. Huang, D. Kasemset, N. Nouri and D. Ackley, J. Electron. Mater. **18**, 603 (1989).
16. T. W. Kim, Y. Kim, S. K. Min, J. Y. Lee and S. J. Lee, Semicond. Sci. Technol. **9**, 1823 (1994).
17. J. R. Botha and A. W. R. Leitch, Appl. Phys. Lett. **63**, 2534 (1993).
18. J. S. A. Adelabu, Appl. Phys. A **62**, 83 (1996).
19. H. Haefner, L. Lehmann, R. Mitdank, G. Oelgart and E. Schulze, Phys. Stat. Sol. (a) **122**, 683 (1990).
20. D. C. Bertolet, J. K. Hsu and K. M. Lau, J. Electron. Mater. **20**, 197 (1991).
21. F. Agahi, C. R. Lutz Jr. and K. M. Lau, J. Cryst. Growth **139**, 344 (1994).
22. H. Kawai, K. Kaneko and N. Watanabe, J. Appl. Phys. **56**, 463 (1984).
23. P. M. Frijlink and J. Maluenda, Japan. J. Appl. Phys. **21**, L574 (1982).
24. T. Fukunaga, K. L. I. Kobayashi and H. Nakashima, Japan. J. Appl. Phys. **24**, L510 (1985).

25. J. Singh, K. K. Bajaj and S. Chaudhuri, Appl. Phys. Lett. **44**, 805 (1984).
26. M. A. Herman, D. Bimberg and J. Christen, J. Appl. Phys. **70**, R1 (1991).
27. Y. Hsu, W. I. Wang and T. S. Kuan, J. Vac. Sci. Technol. B **14**, 2286 (1996).
28. N. Inoue, K. Ikuta, M. Shinohara and J. Osaka, J. Cryst. Growth **146**, 379 (1995).
29. A. R. Smith, K. J. Chao, C. K. Shih, Y. C. Shih, K. A. Anselm and B. G. Streetman, J. Vac. Sci. Technol. B **13**, 1824 (1995).
30. M. T. Furtado and M. S. S. Loural, Braz. J. Phys. **24**, 209 (1994).
31. M. T. Furtado and M. S. S. Loural, in Defect and Diffusion Forum (Scitec Publications, Switzerland) **127-128**, 9 (1995).
32. E. H. Li, B. L. Weiss and K. S. Chan, IEEE J. Quantum Electron. **32**, 1399 (1996).
33. S. M. Wang, T. G. Anderson, W. Q. Chen, U. Sodervall and J. Thordson, J. Cryst. Growth **135**, 455 (1994).
34. D. L. Mathine, G. N. Maracas, D. S. Gerber, R. Droopad, R. J. Graham and M. R. McCartney, J. Appl. Phys. **75**, 4551 (1994).
35. R. Azoulay, B. Jusserand, G. Le Roux, P. Ossart and L. Dugrand, J. Cryst. Growth **77**, 546 (1986).
36. M. Sacilotti, L. Horiuchi, J. Decobert, M. J. Brasil, L. P. Cardoso, P. Ossart and J. D. Garnière, J. Appl. Phys. **71**, 179 (1992).
37. G. Bastard and J. A. Brum, IEEE J. Quantum Electron. **22**, 1625 (1986).
38. G. Bastard, in *Wave Mechanics Applied to Semiconductor Heterostructures* (Les Éditions de Physique, France, 1988).
39. D. J. Ben Daniel and C. B. Duke, Phys. Rev. B **152**, 683 (1966).
40. C. Delalande and G. Bastard, in *Semiconductor Interfaces: Fonnation and Properties* edited by G. Lelay, J. Derrien and N. Bocarra (Springer Verlag, Berlin, 1987) p.340.
41. A. P. French and E. F. Taylor, in *An Introduction to Quantum Physics* (W. W. Norton & Company Inc., New York, 1978) p.174.
42. H. C. Casey and M. B. Panish, in *Heterostructure Lasers Part A*, edited by Y. H. Pao and P. Kelley (Academic Press, New York, 1978) p. 193.
43. R. C. Miller, D. A. Kleinman and A. C. Gossard, Phys. Rev. B **29**, 7085 (1985).
44. M. T. Furtado, M. S. S. Loural and A. C. Sachs, J. Appl. Phys. **62**, 4926 (1987).
45. B. A. Vojak, N. Holonyak Jr., W. D. Laidig, K. Hess, J. J. Coleman and P. D. Dapkus, Solid State Commun. **35**, 477 (1980).
46. J. Decobert, L. Horiuchi, M. A. Sacilotti, M. S. S. Loural, A. C. Lamas and M. T. Furtado, in *Crystal Properties and Preparation*, edited by E. Lendvay (Trans Tech Publications, Zurich) **32-34**, 508 (1991).
47. M.A. Sacilotti and A.C. Bordeaux-Rego, Rev. Fis. Apl. Instr. **4**, 189 (1989).
48. M. S. S. Loural, PhD Thesis (1991), Universidade Estadual de Campinas (unpublished).
49. G. B. Stringfellow, J. Cryst. Growth **137**, 212 (1994).
50. G. B. Stringfellow, J. Cryst. Growth **62**, 225 (1983).
51. H. C. Lee, A. Hariz, P. D. Dapkus, A. Kost, M. Kawase and E. Garmire, Appl. Phys. Lett. **50**, 1182 (1987).
52. K. Fujiwara, N. Tsukada and T. Nakayama, Appl. Phys. Lett. **53**, 675 (1988).
53. E. X. Ping, Appl. Phys. Lett. **62**, 493 (1993).
54. H. P. Hjalmarson, G. D. Gilliland, D. J. Wolford, T. F. Kuech and J. A. Bradley, J. Lumin. **60-61**, 830 (1994).
55. T. E. Schlesinger and T. Kuech, Appl. Phys. Lett. **49**, 519 (1986).
56. S. Schmitt-Rink and C. Ell, J. Lumin. **30**, 585 (1985).
57. C. Delalande, G. Bastard, J. Orgonasi, J. A.

Brum, H. W. Liu, M. Voos, G. Weimann and W. Schlapp, Phys. Rev. Lett. **59**, 2690 (1987).

58. S. B. Ogale, A. Madhukar, F. Voillot, M. Tomsen, W. C. Tang, J. Y. Kim and P. Chen, Phys. Rev. B **36**, 1662 (1987).

59. D. F. Welch, G. W. Wicks and L. F. Eastman, Appl. Phys. Lett. **46**, 991 (1985).

60. D. A. Kleinman and R. C. Miller, Phys. Rev. B**32**, 2266 (1985).